Bulge-to-disk decomposition of 5 ALHAMBRA galaxies in 23 photometric bands

José Concejo[1,2]
[1] Observatorio Astrónomico de la Universidad de Valencia, Spain
[2] Institute of Astronomy of the Bulgarian Academy of Sciences
jconcejo64@hotmail.com
(Research report. Accepted on 20.09.2009)

Abstract. The Advanced Large Homogeneous Area Medium Band Redshift Astronomical Survey (ALHAMBRA Survey) contains images of galaxies obtained through 20 square-like shaped, equal width, medium band filters from 350 nm to 970 nm, plus J, H and K_s standard filters. This survey gives possibilities to determine the morphological parameters for galaxies with $z \approx 0.2$ and to analyze the changes of these ones as a function of the wavelength. To obtain the information related to the morphological parameters of a galaxy it is necessary to extract structural components from galaxy images. This is achieved by using a two-dimensional fitting algorithm called GALFIT whose main characteristics and fitting procedure are briefly exposed in this paper. The present study is based on a simple bulge-to-disc decomposition of the galaxy image and it is focused only on the contribution of each component to the total optical luminosity. Clearly, such a choice is the first step to test the GALFIT possibilities on images of galaxies from the ALHAMBRA Survey. This is illustrated by means of 5 case studies of galaxies with $0.1 \leq z \leq 0.2$, which include 3 spiral galaxies and 2 elliptical galaxies.
Key words: galaxies: morphology

Декомпозиция на балдж и диск на 5 галактики от обзора ALHAMBRA в 23 фотометрични ивици

Хосе Консехо

Обзорът ALHAMBRA съдържа изображения на галактики, получени през 20 П-образни, с еднаква ширина, средноивични филтри от 350 nm до 970 nm, плюс J, H и K_s стандартни филтри. Този обзор позволява определяне на морфологични параметри за галактики със $z \approx 0.2$ и анализ на измененията на параметрите като функция на дължината на вълната. За получаване на информация относно морфологичните параметри на галактиката е необходимо да се извлекат от изображението структурни компоненти. Това се постига чрез прилагане на двумерния фитиращ алгоритъм наречен GALFIT, чиито главни характеристики и фитираща процедура са представени кратко в тази статия. Настоящето изследване е базирано на проста декомпозиция на изображението на галактиката на балдж и диск, като е фокусирано само върху приноса на всеки компонент към пълната оптическа светимост. Този избор е първа стъпка от тест на възможностите на GALFIT за изображения от обзора ALHAMBRA. Това е илюстрирано чрез изследване на 5 галактики със $0.1 \leq z \leq 0.2$, включващо 3 спирални и 2 елиптични галактики.

1 Introduction

Determining galaxy morphology and the associated luminosity is a task that has been performed for over half a century to understand galaxy formation and evolution. The use of theoretical profiles to fit the light distribution

within a galaxy is based on empirical techniques and it follows a permanent progress. Galaxy fitting is undergoing a noticeable change in the last two decades due on one hand to a rapid increase in computer technology (high capacity for calculations and development in programming) and on the other hand to a remarkable improvement of the know-how in building instruments used in observational astronomy in combination with astrophysical techniques that have allowed telescopes to reach an unprecedent accuracy in collecting data (space telescopes, e.g. HST, electronic devices, e.g. CCD imaging in telescopes).

The Advanced Large Homogeneous Area Medium Band Redshift Astronomical (ALHAMBRA) Survey (Moles et al. 2005) is intended to provide a huge collection of photometric data for galaxies up to $z \approx 5$, concerning a few hundred thousands objects.

The preference for the use of GALFIT as the technique to fit the galaxies light profiles is motivated because such a two-dimensional modeling allows to find better true parameter values and also it can take into account isophote twists and ellipticity changes to solve problems such as degeneracies encountered in a one-dimensional fitting procedure.For the purpose of the present study, nearby galaxies ($z \approx 0.2$) have been selected from the ALHAMBRA Survey.

In Section 2 an outline of the ALHAMBRA Survey is presented. Section 3 describes the use of the two-dimensional fitting algorithm GALFIT (Peng et al. 2002), shows the parameters associated to each available profile for fitting light distribution of an astronomical object and considers important remarks about GALFIT. Section 4 gives the results obtained for the 5 case studies of nearby galaxies ($0.1 \leq z \leq 0.2$) using a simple 2-component (B/D) decomposition and provides the contribution of the absolute magnitude of the disc to the total absolute magnitude (bulge + disc) as a function of the wavelength.

2 The ALHAMBRA Survey

2.1 Global scientific aim and opportunity

Cosmic Evolution is one of the main subjects of interest in Cosmology. It is crucial to unravel real cosmic evolution from physical variance at a particular redshift and the details of the metric. A correct treatment to study cosmic evolution requires to consider an important size of physical volumes, including low redshift regions, to accurately measure mean values of physical properties and their variance. It is therefore necessary to define a sample area wide and deep enough associated to a continuous spectral exposure to shun the complexity introduced by selection functions which depend on the redshift and on the nature of the objects. Hitherto the most important surveys have been photometric ones, such as the Sloan Digital Sky Survey (SDSS) which has covered a wide area, or such as the Hubble Deep Field (HDF) which has established a deeper cartography of the distant Universe, but only for small areas.

Combining wide area with depth results is a challenging task. On one side the use of broadband filters supply low precision results to calculate redshifts

and approximate values of the Spectral Energy Distributions (SEDs). On another side spectroscopic surveys provide more accurate data, but cannot reach as deep as photometric surveys and, as they cover small areas, do not span the complex variety of objects in the Universe.

How a photometric study can bring together large and deep area, fine spectral resolution and coverage? The ALHAMBRA Survey is such an answer to the question and covers a four square degree area (sky area covered equivalent to 20 times that of full moon) with 20 contiguous, equal width, medium band optical filters from 350 nm to 970 nm, plus the three standard broad bands, JHK_s, in the Near InfraRed (NIR). Also the ALHAMBRA survey will provide accurate photometric redshifts ($\Delta z < 0.015(1+z)$) and SED classification for more than 300,000 galaxies and Active Galactic Nuclei (AGNs).

Table 1. Central wavelength λ_c for the ALHAMBRA Survey filter system.

No.	λ_c nm	No.	λ_c nm
01	365.5	11	675.5
02	396.5	12	706.5
03	427.5	13	737.5
04	458.5	14	768.5
05	489.5	15	799.5
06	520.5	16	830.5
07	551.5	17	861.5
08	582.5	18	892.5
09	613.5	19	923.5
10	644.5	20	954.5

The central astronomical objective of the ALHAMBRA Survey is to provide the community with a set of data appropriate for the systematic study of Cosmic Evolution. The intention is to materialize a foliation of the space-time, producing narrow slices in the z-direction whereas the spatial sections are large enough to be cosmologically representative, what could be called Cosmic Tomography.

2.2 The ALHAMBRA Survey filter system

For a complete understanding of the choice of the ALHAMBRA Survey filter system, please refer to Moles et al. 2005; Fernández-Soto et al. 1999; Benítez 2000; Benítez et al 2004.

The optimum and most efficient filter system has been designed to fulfill two important characteristics: a) to get accurate SED and z determination for the largest possible number of objects, for a given total amount of observing time, and b) to be sensitive to relatively faint emission lines. Thus the ALHAMBRA Survey filter system is composed by 20 contiguous, medium-band, FWHM = 31 nm, square-like shaped filters with marginal overlapping in λ, covering the complete optical range from 350 nm to 970 nm. The central

wavelength λ_c for each filter are given in Table 1 and transmission curves are shown in Fig.1.

2.3 Field selection

Although the Universe is in principle homogeneous and isotropic at large scale, the astronomical objects are clustered in the sky on different scales. These clusters contain a rich information about the structure formation process, that is about evolution. To study this evolution, the ALHAMBRA Survey must cover the largest number of scales.

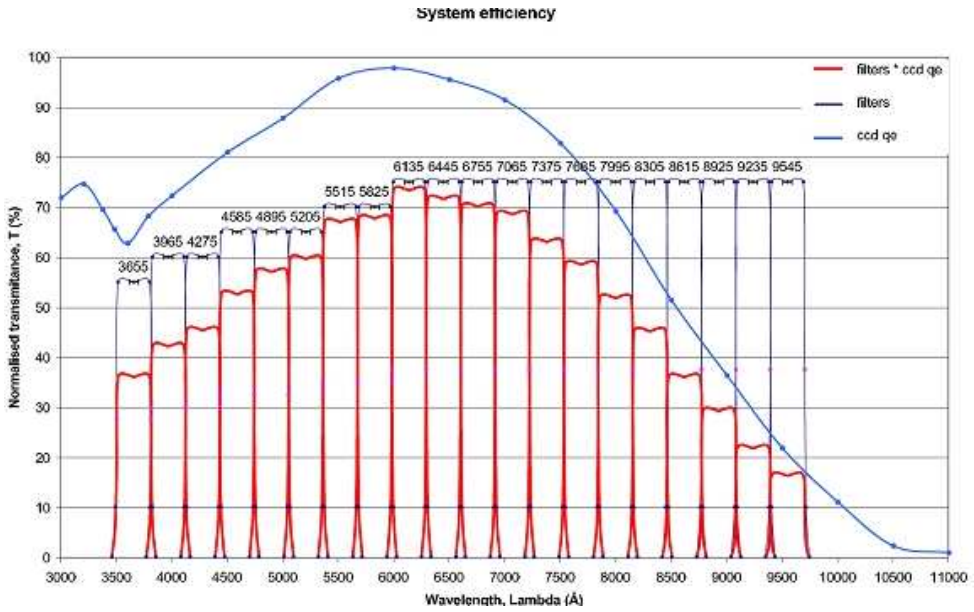

Fig. 1. Calculated transmission curves of the ALHAMBRA Survey taking into account the atmospheric transmission and the CCDs quantum efficiency for the minimum filter transmission guaranteed by the manufacturer.

Measuring a population of a certain volume density is a Poissonian process with an associated variance. Different densities of the same population would be obtained when measuring at different places. The variance in those measurements is dictated by the volume density of the population under study, the volume searched and the clustering of the population. To eliminate this cosmic variance the survey must be based on independent volumes.

A balance must exist between probing contiguous and independent areas. This is the reason why for the ALHAMBRA Survey a total area of four square degrees, divided in eight different fields, has been defined. The diversity of fields will ensure the necessary independence between the volumes to reduce the cosmic variance, and at the same time each field will be based on observations within two strips of $1^o \times 0.25^o$ to ensure the contiguity condition.

Also the selection of the fields must ensure the following criteria: low (galactic) extinction, no (or few) known bright sources, high galactic latitude, overlap with other surveys and/or other wavelengths. Table 2 presents the ALHAMBRA Survey fields selected.

Table 2. The ALHAMBRA Survey fields. Additional information is the name of other surveys of interest that overlap the field.

Field name	RA (J2000)	DEC (J2000)	100 μm	E(B − V)	l deg	b deg
ALHAMBRA-1	00 29 46.0	+05 25 28	0.83	0.017	113	-57
ALHAMBRA-2/DEEP2	02 28 32.0	+00 47 00	1.48	0.031	166	-53
ALHAMBRA-3/SDSS	09 16 20.0	+46 02 20	0.67	0.015	174	+44
ALHAMBRA-4/COSMOS	10 00 28.6	+02 12 21	0.91	0.018	236	+42
ALHAMBRA-5/HDF-N	12 35 00.0	+61 57 00	0.63	0.011	125	+55
ALHAMBRA-6/GROTH	14 16 38.0	+52 25 05	0.49	0.007	95	+60
ALHAMBRA-7/ELAIS-N1	16 12 10.0	+54 30 00	0.45	0.005	84	+45
ALHAMBRA-8/SDSS	23 45 50.0	+15 34 50	1.18	0.027	99	-44

2.4 Instruments

For a detailed information on the instruments used in the ALHAMBRA Survey please see the following websites:

http://alhambra.iaa.es:8080/alhambra/

http://www.caha.es/CAHA/Instruments/LAICA/index.html

http://www.mpia-hd.mpg.de/IRCAM/O2000/index.html

In the optical range (covered by the 20 contiguous filters) the camera used is Large Area Imager for Calar Alto, LAICA. LAICA is installed at the prime focus of the 3.5 m telescope at Calar Alto Observatory, Almería, Spain. Due to the specific design/arrangement of the camera, series of 4 exposures has to be taken to fill the gaps between the 4 CCDs although the advantage of this specific arrangement is that it makes full use of the sensitive area: the filling factor is 100%. A further advantage is that 4 single small filters can be used (instead of a single large one) which are much easier available and cheaper. The main disadvantage of this arrangement is enhancement of image distortion effects; this implies a precise treatment during image reduction.

Table 3. Basic characteristics of the used CCD cameras.

Camera	LAICA	OMEGA2000
Telescope	3.5 m Calar Alto	3.5 m Calar Alto
Field of view	44.36x44.36 arcmin	15.4x15.4 arcmin
Pixel scale	0.225 arcsec/pixel	0.45 arcsec/pixel
Detector	4 CCD, 4096x4096 pixels	HAWAII-2, 2048x2048 pixels

In the NIR range (covered by standard filters JHK_s) the camera used is OMEGA 2000. Omega 2000 is a prime focus near infrared wide field camera for the 3.5m telescope at Calar Alto Observatory, Almería, Spain.

Considering the goals of the Survey, the characteristics of the instruments LAICA and OMEGA 2000, and the average conditions in Calar Alto and, more specifically, at the 3.5m dome, the following limiting conditions have been adopted to get data: limit value for Seeing is 1.2 arcsec in the optical range and 1.4 arcsec in the NIR. Basic characteristics of both cameras, LAICA and OMEGA 2000 are shown in Table 3.

3 Two-dimensional fitting algorithm GALFIT

For a complete description of GALFIT, please refer to Peng et al. (2002) or GALFIT Home Page at: http://users.ociw.edu/peng/work/galfit/galfit.html

3.1 Introduction

GALFIT is an algorithm that analyses the light profile of astronomical objects and fits them with one or several two-dimensional parameterized, axisymmetric, functions. Each function is defined by a set of free fitting parameters that are modified to coincide with the light distribution of an image; multiple functions can be adjusted simultaneously.

There are four input images for GALFIT: the CCD image of the galaxy, a noise array, a PSF, and an optional dust (or bad pixel) mask [respectively labels A), C), D) and F) in Table 4].

To find the best fit, GALFIT minimizes the reduced χ^2 between the data of the image and the model, adjusting the free parameters at once. This is achieved through a modified Levenberg-Marquardt (L-M) algorithm (downhill gradient), taken from Numerical Recipes. This type of algorithm is one of the fastest to find minima in many parameters spaces. The reduced χ^2 is defined in the standard way by

$$(1)\ \chi^2_\nu = 1/N_{dof} \times \sum\sum[(flux_{x,y} - model_{x,y})^2/\sigma^2_{x,y}],$$

where $flux(x, y)$ is the data at pixel (x, y), $model(x, y)$ is a value that GALFIT generates at (x, y), and σ(x,y) on the denominator is the Poisson deviate of the flux at (x, y). $Sigma(x, y)$, is what is known in GALFIT as the "sigma image" in which the pixel values are Poisson deviates corresponding to flux in the data image, at the same (x, y) position. GALFIT computes χ^2_ν and uses the definition of sigma in the standard way.

3.2 Physical parameters

GALFIT looks for four parameters in the image header:

1.- EXPTIME - exposure time of the image

2.- GAIN (or ATODGAIN) - in units of electrons / ADU (Analogue to Digital Units)

3.- RDNOISE - reading noise of the image in units of electrons
4.- NCOMBINE - number of combined images

EXPTIME is used to calculate the magnitude of the object and the surface brightness of the fit. GAIN, RDNOISE and NCOMBINE are only used to assign a weight to each pixel in the fit based on a Poissonian noise model. The value of the sigma image can also be directly given as input by the user.

3.3 Analytical parameters

Geometrical parameters. In GALFIT all the profiles are axially symmetric, generalized ellipses. The radial distance of a pixel (x, y) to an object centered at (x_c, y_c) is defined by

$$(2)\ r = (|x - x_c|^{c+2} + |(y - y_c)/q|^{c+2})^{1/(c+2)}$$

and the principle axes of the ellipse are aligned with the coordinate axes. The free parameter c controls the shape of the isophote; for $c = 0$ the isophote is an ellipse, for $c > 0$ the isophote has a boxy shape and for $c < 0$ the isophote has a disky shape. In equation (2) the parameter q is the ratio of the minor to major axis of an ellipse.

Figure 2 shows two examples of azimuthal shapes as a function of c for $q = 1.0$ and $q = 0.5$. The position angle (PA), that is the orientation of the major axis of the ellipse, and the coordinates of its centre are the other free parameters. In total there are 5 free parameters.

Profile Parameters. Here only a brief description of the different profiles is presented. For more details, please to Peng et al. (2002) or GALFIT Home Page at: http://users.ociw.edu/peng/work/galfit/galfit.html, Kormendy & Bruzual 1978; Shaw & Gilmore 1989; Kent, Dame, & Fazio 1991; Andrekakis & Sanders 1994.

GALFIT offers the possibility of using several functions to fit galaxy profile. However, in this study only two of the profiles (Sérsic and Nuker) have been selected as a first approach to obtain a B/D decomposition.

The Sérsic profile. It is a power law that has the following form

$$(3)\ f_r = f_e exp[-k(r/r_e)^{1/n} - 1)],$$

where r_e is the effective radius of the galaxy, f_e is the surface brightness at r_e, n is the power-law index (also known as the concentration parameter), and k is coupled to n such that half of the total flux is always within r_e.

Bulges may be represented either by the de Vaucouleurs (1948) profile or by exponential profiles, which are indeed special cases of the more general Sérsic profile. In fact the Sérsic profile forms a continuous sequence from a Gaussian ($n = 0.5$) through an exponential ($n = 1$) to a de Vaucouleurs ($n = 4$) profile simply by varying the exponent.

The flux, integrated over all radii for an elliptical Sérsic profile with an axis ratio q, is

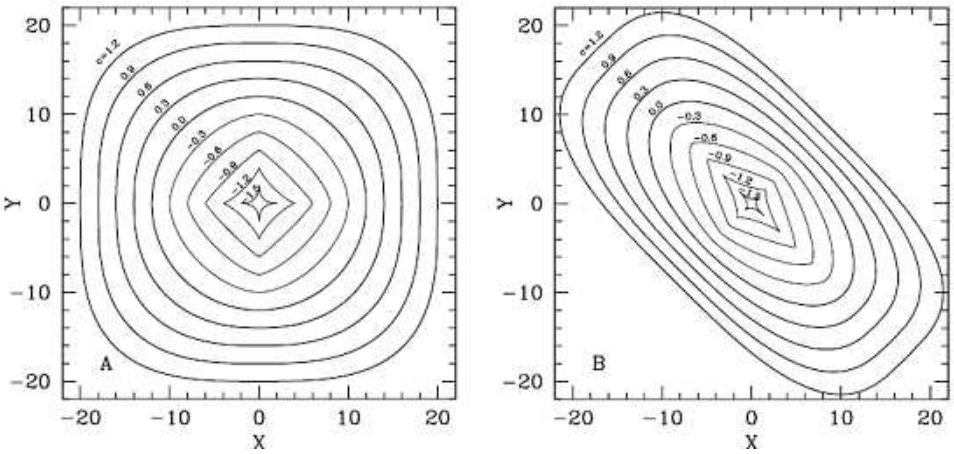

Fig. 2. Azimuthal shape of ellipses based on Equation (2), centered at $x_c = y_c = 0$ and applied for two different axis ratios: $q = 1$ (left panel) and $q = 0.5$ (right panel), as a function of the diskiness/boxiness parameter c.

(4) $F_{tot} = 2\pi r_e^2 f_e exp^k nk^{-2n} \Gamma(2n) q/R(c)$,

where $\Gamma(2n)$ is the gamma function and $R(c)$ is a function that accounts for the area ratio between a perfect ellipse and a generalized ellipse of diskiness/boxiness parameter c, given by

(5) $R(c) = \pi(c+2)/[4\beta(1/(c+2), 1+1/(c+2))]$,

where $\beta(1/(c+2), 1+1/(c+2))$ is the "beta" function with two arguments. It should be noted that F_{tot} is fitted instead of f_e because F_{tot} is a more useful parameter. F_{tot} is converted into a magnitude by GALFIT using the standard FITS exposure time parameter (EXPTIME) in the image header ($m_{tot} = -2.5log_{10}(F_{tot}/t_{exp}) + m_0$).

The Sérsic model has eight free parameters : $x_c, y_c, m_{tot}, r_e, n, q, PA, c$.

The Gaussian profile. This is a special case of the Sérsic profile with $n = 0.5$, and instead of using r_e to characterize the size of an object, here the parameter is Full Width at Half Maximum, $FWHM = 2.356\sigma$. The functional form is

(6) $f_r = f_0 exp(-r^2/2\sigma^2)$,

and the flux is

(7) $F_{tot} = 2\pi\sigma^2 f_0 q R(c)$.

The Gaussian model has seven free parameters: $x_c, y_c, F_{tot}, r_e, \sigma, q, PA, c$.

The Nuker Law. It was introduced by Lauer et al. (1995) to fit the nuclear profile of nearby galaxies and it has the following form

(8) $I_r = I_b 2^{(\beta-\gamma)/\alpha}(r/r_b)^{-\gamma}[1+(r/r_b)^{-\alpha}]^{(\beta-\gamma)/\alpha}$.

This is a double-power law and it has five adjustable parameters: I_b, r_b, α, β, γ. The break radius r_b is the location where the profile changes slope, I_b is the surface brightness at r_b. In GALFIT, the surface brightness magnitude μ_b is fitted instead of I_b and the following relation is used:

(9) $\mu_b = -2.5 \times log_{10}[I_b/(t_{exp}\Delta x \Delta y)] + \mu_0$.

The two-dimensional Nuker profile has a total of ten free parameters: $x_c, y_c, I_b, r_b, \alpha, \beta, \gamma, c, q, PA$.

The background sky. GALFIT also allows to fit the background sky of the image. In GALFIT, the sky can be characterized by gradient variation in the x and/or y directions. The geometrical centre of the image (x_0, y_0) is a fixed position and serves to compute the background level via

(10) $sky(x,y) = sky(x_0,y_0) + (x-x_0) \times \partial[sky]/\partial x + (y-y_0) \times \partial[sky]/\partial y$.

The background fitting has a total of three free parameters: $sky(x_0, y_0), sky|_x$ and $sky|_y$.

3.4 Using GALFIT

For a complete description of GALFIT, please refer to Peng et al. 2002 or GALFIT Home Page at:http://users.ociw.edu/peng/work/galfit/galfit.html

In GALFIT the parameters can be input manually or in an interactive way via an input file (see Table 4). Due to the large amount of parameters the latter is higly recommended. In the input file, anything preceeded by # (comment) as well as the blank lines are ignored by the program. It is essential to correctly introduce the parameters in the input file as if there is any typing mistake, GALFIT will keep on running without popping-up any error and this can lead to unusual results.

The input file for GALFIT has two sections: a section with the parameters relating to the image, CCD image of the galaxy, a noise array, a PSF, and an optional dust (or bad pixel) mask, and a section relating to the object(s) within the image, position x, y, PA, axis ratio, diskiness/boxiness. The parameters relating to an object can be either fixed or free for the fit. In the latter section it is to be noticed that there is always an object that represents the sky. Also in this same section, it is where the components are specified; for a B/D decomposition two objects are specified, one as "bulge" and the other as "disc", and both have their centre coordinates [label 1) in Table 4] fixed at the same position in the image. The decomposition lies in that a different profile is assigned to each of the two components.

Table 4. Example of an input file used in GALFIT showing two sections: IMAGE PARAMETERS and FITS PARAMETERS.

–	IMAGE PARAMETERS ——	
A)	image.fits	# Input data image (FITS file)
B)	imgblock.fits	# Name for the output image
C)	none	# Noise image name (made from data if none or blank)
D)	psfdepalo.fits	# Input PSF image and (optional) diffusion kernel
E)	1	# PSF fine sampling factor relative to data
F)	dust.fits	# Pixel mask (ASCII file or FITS file with non-0 values)
G)	none	# File with parameter constraints (ASCII file)
H)	150 250 420 520	# Image region to fit (xmin xmax ymin ymax)
I)	80 80	# Size of convolution box (x,y)
J)	26	# Magnitude photometric zeropoint
K)	0.025 0.025	# Plate scale (dx dy) [arcsec/pix. Only for Nuker]
O)	both	# Display type (regular, curses, both)
P)	0	# Create output image only? (1=yes, 0=optimize)
S)	0	# modify/create objects interactively?
–	FITS PARAMETERS	# – Object number : 1
0)	Sérsic	# Object type
1)	200 315 1 1	# position x, y [pixel]
3)	22.00	# total magnitude
4)	10	# R_e (half-light radius) [pixels]
5)	4 1	# Sérsic exponent (deVaucouleurs=4)
8)	0.75	# axis ratio (b/a, 1 for circle, ¡1 for ellipse)
9)	-5.0	# position angle (PA) [Degrees : Up=0, Left=90]
10)	0.5	# diskiness (-) or boxiness (+)
Z)	0	# output option (0 = resid., 1 = Don't substract)
–	FITS PARAMETERS	# Object number : 2
0)	sky	# Object type
1)	1.40	# sky background at center of fitting region [ADUs]
2)	0.00	# dsky/dx (sky gradient in x)
3)	0.00	# dsky/dy (sky gradient in y)
Z)	0	# output option (0 = resid., 1 = Don't substract)

3.5 Limitations and remarks concerning the use of GALFIT

Here specific particularities are given.

1. GALFIT can compute profiles for several objects of the same image at once. However, this requires a relatively long time and sometimes leads to a computing error; but this also depends on the computer capacities.

2. For the study of objects like nearby galaxies GALFIT needs a manual feeding by the user to set up the parameters and the initial data of each object of an image.

3. The program does not pop-up information enough when an error comes off. This implies time consuming to detect the causes of the error.

4. A detailed fitting procedure should be followed, especially in the case of the study of nearby galaxies when trying to obtain a B/D decomposition.

It is important to notice that a simple one or two component fits frequently produce large residuals that have bipolar or quadrupolar symmetry, which can be reduced with additional components (3 to 5 in total). Even so, as the purpose of the study that is presented here is intended to provide a first approach in using GALFIT, a simple B/D decomposition is used.

4 Results for 5 cases studies

4.1 Preliminary tests

Series of tests using Sérsic (includes Exponential, Gaussian and de Vaucouleurs) and Nuker profiles has been done repeatedly for each of the preliminary test, but in this paper only two examples are shown.

For a correct use of GALFIT, it was first decided to carry out a couple of preliminary tests on two selected objects (galaxies) of the ALHAMBRA Survey. The use of various models, applied to these objects, will reveal crucial information for determining the influence of the different parameters in each case. This will serve in deciding which profiles could better fit a B/D decomposition. Such a separation between components can also arise in the case of elliptical galaxies formed from mergers (simulations predict that ellipticals should contain a significant embedded stellar disk component; Naab & Burkert 2001).

For this preliminary study, the laws used are the Sérsic (which includes as special cases Gaussian, $n = 0.5$; Exponential, $n = 1$; de Vaucouleurs, $n = 4$) and the Nuker, as all other available profiles (in GALFIT) are adequate for fitting light distribution of non-compact objects (such as globular clusters).

The best fit of the profile for a chosen object is based on two considerations: first, the value of the reduced χ^2 can vary between 1 and 10^5, but should be as close as possible to 1 (Peng et al. 2002) and second, looking carefully at each of the computed images (specially the residuals) to determine whether these ones do approach the original image of the object.

First Test. Sérsic profile and Nuker law are applied on three images of a galaxy obtained through the filters 458, 644 and 861 nm; this ensures a large spectral coverage and it is relatively easy to get a first estimation for a B/D decomposition. An example is shown in Fig.3.

Second Test. Under the same conditions as in the First Test, a galaxy and a foreground star are fitted together: this serves to evaluate the capacity of GALFIT to separate adequately these two very close objects and to compute the related profiles simultaneously. An example is shown in Fig.4.

The preliminary tests have shown that the Nuker law is not well suited for a B/D decomposition (GALFIT collapses in the attempt to fit with a Nuker law the two components for the spiral galaxy showed in Fig.3). The residuals obtained in Fig.3 and 4 show a bipolarity which could be expected (remember 3.5., point 4.).

Figure 4, Central panel, clearly shows that GALFIT has proven its ability in computing simultaneously profiles of two very close objects.

4.2 Selecting objects

The objects chosen for the present study are 5 galaxies, 3 spiral galaxies and 2 elliptical ones, with $0.1 \leq z \leq 0.2$ (see Fig. 5 and 6), belonging to the ALHAM-BRA-8 field (see Table 2). The size of these 5 galaxies is relatively large when compared to all other objects appearing in the same images. Consequently a more accurate fitting of the isophotes is necessary. This will

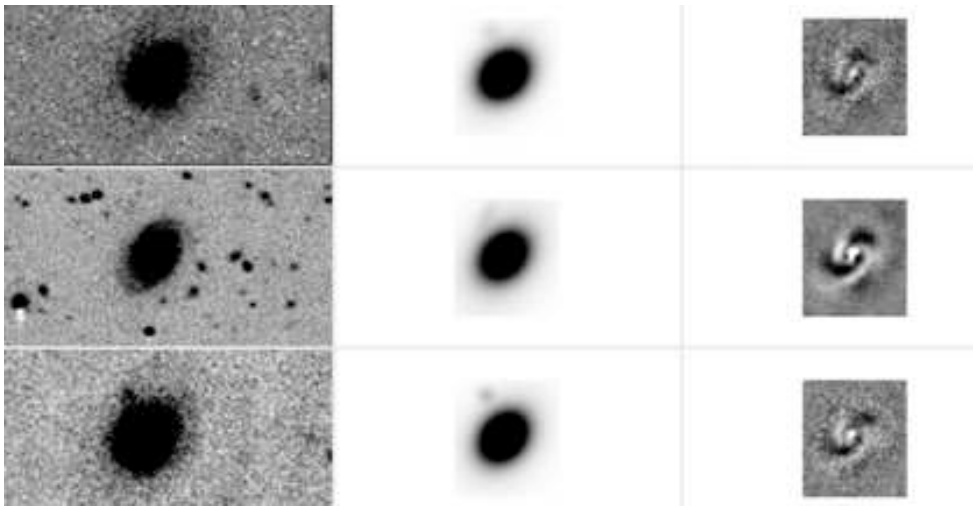

Fig. 3. Left panel: Original image of a spiral galaxy through the filters 458, 644 and 861 nm. Central panel: Computed model for a Sérsic profile case. Right panel: Residuals (difference between the original image and the computed model).

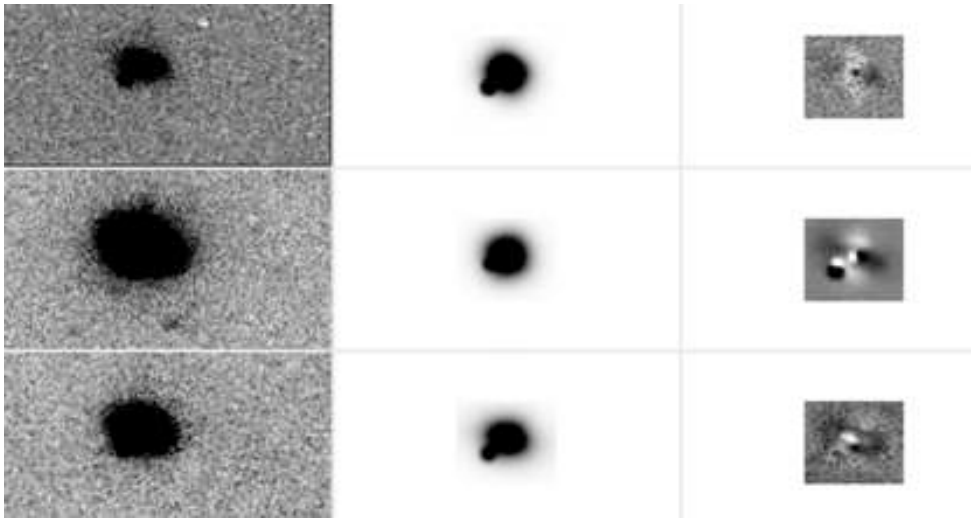

Fig. 4. Left panel: Original image of an elliptical galaxy with a very close foreground star through the filters 458, 644 and 861 nm. Central panel: Computed model for a Nuker profile fitting for the galaxy and a Gaussian profile fitting for the foreground star. Right panel: Residuals (difference between the original image and the computed model).

produce a relatively wide range of values of the reduced χ^2 (but still acceptable for a first evaluation), that is more significant residuals. Nevertheless, this first examination will reveal the tendency of the evolution of the absolute magnitude of the studied objects with the wavelength.

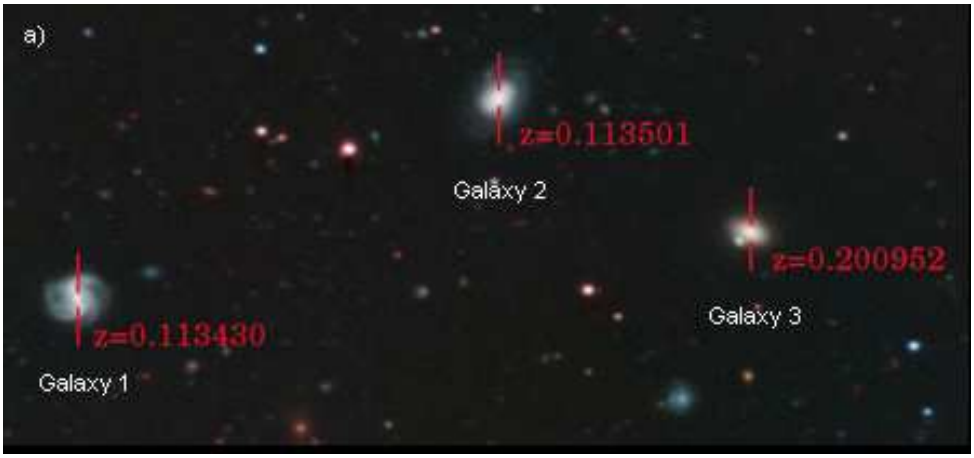

Fig. 5. Image of the studied galaxies 1, 2 and 3 combined from 14 out of the 23 ALHAMBRA filters, those with walengths between 396 nm and 799 nm. The images have been processed aiming to reproduce the real human sensitivity to the objects colours. Hence, each filter has been assigned a different colour tuned to the sensitivity curves of the human eye, with the range 700-800 nm taken as pure red for reference. When the images are integrated, three composites are created, corresponding to the three basic colours (red, green and blue). Processing of the images has been performed with PixInsight Standard. The image span is 3.36'x1.62' and is a reduced patch of the original image of the ALHAMBRA-8 field that span 15'x15'.

The 5 selected galaxies can be identified via their Right Ascencion (RA) and Declination (DEC) coordinates (values directly obtained from the FITS images). Properties of each galaxy can be easily verified because the ALHAMBRA – 8 field overlaps with SDSS (which gives spectroscopic data), thus ensuring that the results obtained in the present study seem correct.

4.3 Choosing profiles

The selected profile for the study of the 5 galaxies is the Sérsic one. From the preliminary tests the Nuker law is discarded.

As mentioned in the introduction of this article, for the studied galaxies, the main aim focuses on getting a B/D decomposition when the used model can guarantee it. In this way, restrictions are established on the possible values for the Sérsic indices. For the case $n = 1$ (exponential law), the profile describes the distribution of isophotes for a disc. For the case $n = 4$ (de Vaucouleurs) the profile describes the distribution of isophotes for a bulge.

Fig. 6. Image of the studied galaxies 4 and 5. Please, see the caption of Fig.5

Restrictions are introduced in GALFIT via an ASCII file that is then indicated in the Image Parameters section under label G (see Fig. 3).

Sérsic profile with restrictions on indices. For the study of the 5 selected galaxies, in the input file data of GALFIT, an object (with its centre coordinates in the image) is introduced with a characteristic of bulge and another object (with the same centre coordinates as the first one) with a characteristic of disc. This translates into values for a Sérsic index varying between 0.5 and 1.5 for the determination of a disc, and between 3.5 and 4.5 for the determination of a bulge.

To compute the contribution of each component, bulge and disc, to the total flux (in the optical range), reminding the relation between the absolute magnitude M and the flux Φ for the disk and the bulge as

(11a) $M_B = -2.5 \times log_{10}\Phi_B + K$ and

(11b) $M_D = -2.5 \times log_{10}\Phi_D + K$,

and working out equations (11a) and (11b), it is easy to establish the expression which gives the percentage of the disc that participates in the total emitted flux by the object. The following relation is obtained

$$(12)[\Phi_D/(\Phi_D + \Phi_B)] \times 100\% = [10^{-0.4M_D}]/[10^{-0.4M_D} + 10^{-0.4M_B}] \times 100\%$$

Sérsic profile without restrictions on indices. In this case, the study of the 5 galaxies proceeds exactly in the same way as for the previous case, except that no restricitions are imposed on the Sérsic indices. The values obtained for these indices will indicate on one hand if the profiles can better fit the light distribution of the object and, on another hand, if it is adequate to

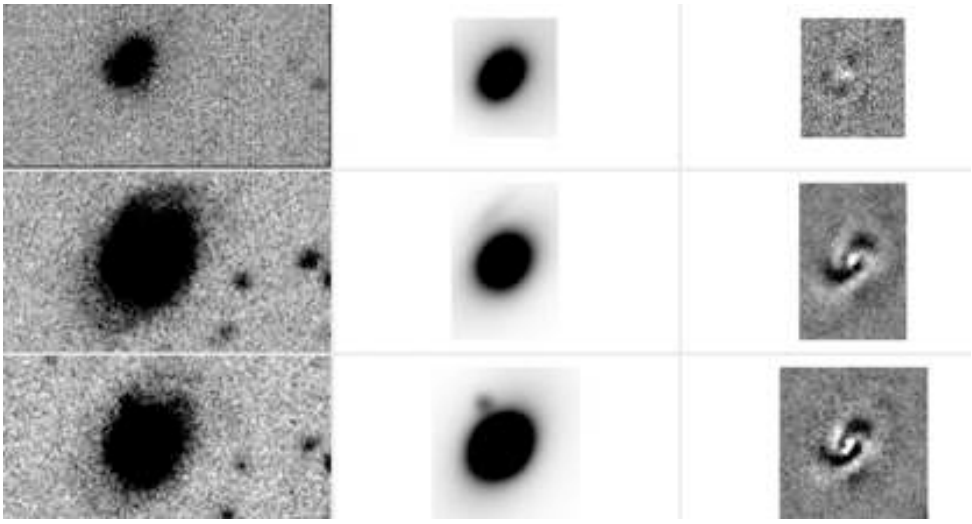

Fig. 7. Left panel: Original image of galaxy 2 through the filters 365, 520 and 768 nm. Central panel: Computed model for a Sérsic profile with restrictions on the indices to fit a bulge ($3.5 \leq n \leq 4.5$) and a disc ($0.5 \leq n \leq 1.5$). Right panel: Residuals (difference between the original image and the computed model).

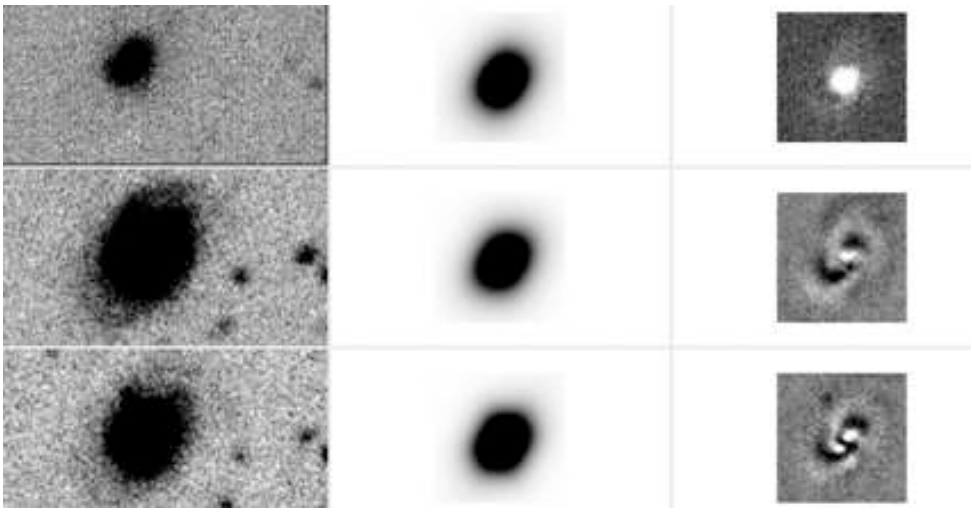

Fig. 8. Left panel: Original image of galaxy 2 through the filters 365, 520 and 768 nm. Central panel: Computed model for a Sérsic Profile without restrictions on the indices to fit a bulge and a disc. Right panel: Residuals (difference between the original image and the computed model).

consider that the total flux emitted by the object corresponds to a "real" B/D decomposition.

4.4 Results

In this paper some examples are presented to illustrate the results, as the complete set of results could result extremely cumbersome. For more information, please contact the author at: jconcejo64@hotmail.com.

For the Sérsic Profile, with and without restrictions on indices, the residuals obtained are very similar and are acceptable for a first trial on the studied objects of the ALHAMBRA Survey. This is illustrated with an example in Fig. 7 and 8, where the original image of the galaxy spans 24" x 15".

For the case of the 3 spiral galaxies, the contribution of the disc to the total flux decreases with the wavelength. This tendency is also noticed for the case of the 2 elliptical galaxies, but the effect is less pronounced because in this case the stellar disc component is embedded.

Figure 9 shows an example of the evolution versus the wavelength of the flux contribution of the disc for the 5 galaxies in the case of a Sérsic Profile with restrictions on the indices to fit a bulge ($3.5 \leq n \leq 4.5$) and a disc ($0.5 \leq n \leq 1.5$). The data are given in Table 5.

Also, the contribution (in percentage) of the disc (or bulge) component to the total emitted flux gives information about the morphological type of the galaxy and the quantity and types of main stars present in the disc (or bulge). In the case of the 5 galaxies studied here, the morphological type extracted from the results are in accordance with the ones assigned by SDSS.

The 3 spiral galaxies of the present study are practically face-on and the surface brightness should be fitted by an exponential law (i.e. with a Sérsic index n = 1). Nevertheless, the data obtained from GALFIT computing show that, when the light distribution is fitted by a Sérsic profile without restrictions on the indices (that is when the Sérsic indices can take free values), although the Sérsic index associated to a disc component moves approximately around a value close to 1, the Sérsic index related to a bulge component fluctuates in a wide range of values (see Table 5). This important fluctuation reflects the (obvious) fact that the simple 2-component (B/D) fit is a basic analysis: the light distribution profiles of the galaxies might be better described if adding components (e.g. like a bar oriented on the 5-11 o'clock direction for galaxy 5, see Fig. 6). This is also confirmed by the residuals obtained for the 3 spiral galaxies, e.g. Right panel in Fig. 7 and 8, which, apart from an expected bipolar symmetry, clearly show a complex spiral structure of galaxy 2 that cannot be evaluated from the image in Fig. 5).

In the case of the 2 elliptical galaxies, the change of the ellipticity of the bulge (i.e. the set of the elliptical isophotes) depends on the distance to the centre of the galaxy. This adds to the difficulty in obtaining a good fit, no matter which profile is computed. Furthermore, there are two different structural types (in terms of components) of elliptical galaxies: some present a relatively simple light distribution that can be easily fitted, but other ones might contain a core (central part) that a Nuker law can fit well, but the same law fails in adjusting the outer parts.

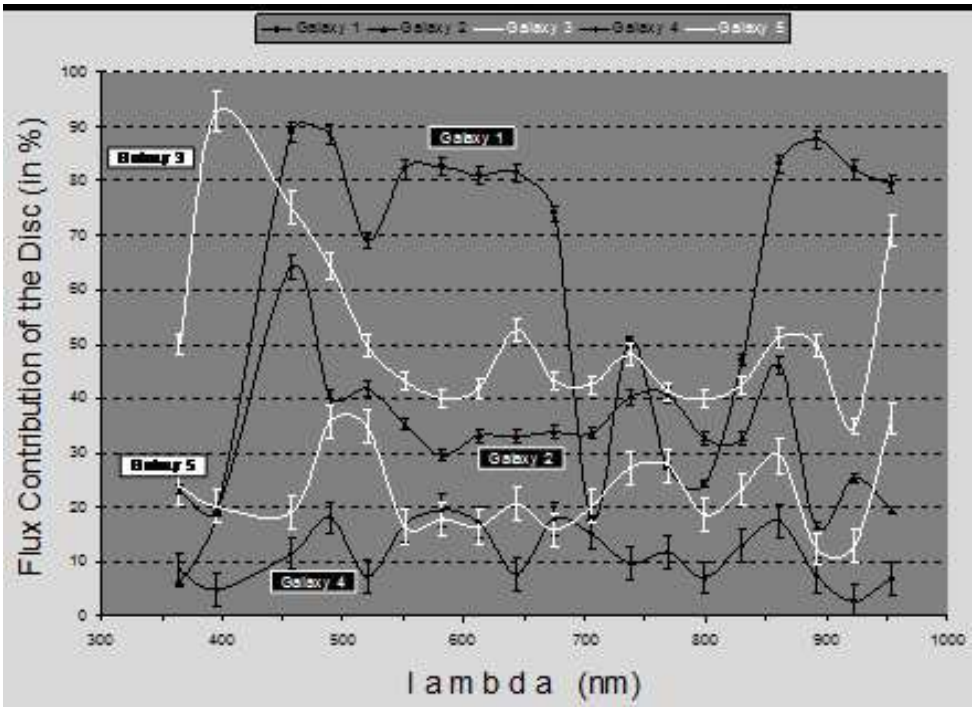

Fig. 9. Evolution as a function of lambda of the flux contribution of the disc (in percentage) for Galaxies 1, 2, 3 (spirals), 4, 5 (ellipticals) computed for a Sérsic profile with restrictions on indices. Black/white solid lines are marked for guidance between the discrete values.

Summary

GALFIT, a general algorithm to decompose a galaxy into various structural components in two dimensions, was tested on 5 galaxies (3 spirals and 2 ellipticals) taken from the ALHAMBRA Survey. An overview of the ALHAMBRA Survey and a brief presentation of GALFIT was then exposed. After proceeding with a couple of preliminary tests using GALFIT on data from the ALHAMBRA Survey, different profiles were applied to 5 cases to obtain a B/D decomposition and to extract the evolution with the wavelength of the absolute magnitude of the disc component.

The results showed that for the Sérsic profile, imposing restrictions on the indeces allowed a relatively good fit for bulge and disc components. Additionally, it was found that the contribution of the disc to the total emitted flux seems to decrease with the wavelength: this could be confirmed by obtaining a better fit (input of the true PSF, largest possible size of the image region and pixel mask). This gave information on the morphological type for each studied galaxy. Also, the selection of the different profiles illustrated that a simple 2-component decomposition was a first approach to extract

Table 5. Sérsic indices conmputed for B/D decomposition in the case of a Sérsic profile without restrictions.

λ, nm	D_1	B_1	D_2	B_2	D_3	B_3	D_4	B_4	D_5	B_5
365	1.24	1.14	1.5	4.6	2.13	2.89	1.24	1.14	1.50	4.60
396	0.54	2.00	1.08	1.68	1.91	4.45	0.54	2.00	1.08	1.68
458	0.31	0.05	0.61	0.94	1.32	5.20	0.31	0.05	0.61	0.94
489	0.53	0.23	1.83	0.56	0.84	3.08	0.53	0.23	1.83	0.56
520	0.55	0.23	1.01	1.19	0.92	0.98	0.55	0.23	1.01	1.19
551	0.72	0.23	0.61	2.39	0.7	3.56	0.72	0.23	0.61	2.39
582	0.35	0.44	1.05	1.84	0.78	1.98	0.35	0.44	1.05	1.84
613	0.37	0.50	0.98	3.07	0.75	2.35	0.37	0.50	0.98	3.07
644	0.41	0.59	1.26	0.20	0.72	1.79	0.41	0.59	1.26	0.20
675	0.36	0.55	0.45	1.78	0.71	2.26	0.36	0.55	0.45	1.78
706	0.36	0.51	1.03	1.14	0.75	1.33	0.36	0.51	1.03	1.14
737	0.33	0.52	0.40	1.71	0.70	1.60	0.33	0.52	0.4	1.71
768	0.66	0.28	0.64	2.00	0.75	1.73	0.66	0.28	0.64	2.00
799	0.70	0.31	0.80	2.86	0.70	2.68	0.70	0.31	0.80	2.86
830	0.71	0.29	0.79	2.30	0.82	2.10	0.71	0.29	0.79	2.30
861	0.59	0.32	0.66	1.87	0.69	3.27	0.59	0.32	0.66	1.87
892	1.13	0.22	1.83	0.97	0.78	7.08	1.13	0.22	1.83	0.97
923	0.60	6.55	0.69	4.41	0.72	8.72	0.60	6.55	0.69	4.41

structural components from galaxy images. Actually it allowed to reveal that other features might be present in the detailed structure of the galaxies.

To confirm this morphological complexity, more accurate fits could be used by introducing more components (such as bars, nuclear point sources). Apart from the absolute magnitude, other morphological parameters can be extracted using GALFIT and then a correlation among them could be established. Eventually the evolution of these morphological parameters with the redshift could be traced, which would bring additional information about cosmic evolution of the universe.

Acknowledgements. I would like to thank Tsvetan Georgiev and Boyko Mihov for their helpful suggestions. This research was made partially with the support of the Grant DO 02-340 of the National Science Foundation in Bulgaria.

References

Ajhar, E. A., Lauer, T. R., Tonry, J. L., Blakeslee, J. P., Dressler, A., Holtzman, J. A., & Postman, M. 1997, AJ, 114, 626
Andredakis, Y. C., & Sanders, R.H. 1994, MNRAS, 267, 283
Benítez, N., 2000, ApJ, 536, 571
Benítez, N. et al, 2004, ApJS, 150, 1
Burstein,D. 1979, ApJ, 234, 829
de Vaucouleurs, G. 1948, Ann. d'Astrophys., 11, 247
de Vaucouleurs, G., de Vaucouleurs, A., Corwin, J. R., Buta, R. J., Paturel, G., & Fouqué, P. 1991, Third Reference Catalogue of Bright Galaxies (New York: Springer)
Dressler, A. 1980, ApJ, 236, 351
Dressler, A., Lynden-Bell, D., Burstein, D., Davies, R. L., Faber, S. M., Terlevich, R., & Wegner, G. 1987, ApJ, 313, 42
Fernández-Soto, A., Lanzetta, K.M., Yahil, A., 1999, ApJ, 513, 34

Freeman, K. C. 1970, ApJ, 160, 811
Ho, L. C. 1999, ApJ, 516, 672
Ho, L. C., Filippenko, A. V., & Sargent, W. L. W. 1997a, ApJ, 487, 568
Ho, L. C., Filippenko, A. V., Sargent, W. L. W., & Peng, C. Y. 1997b, ApJS, 112, 391
Ho, L. C., & Peng, C. Y. 2001, ApJ, 555, 650
Ho, L. C., et al. 2000, ApJ, 541, 120
Jedrzejewski, R. 1987, MNRAS, 226, 747
Kent, S. M., Dame, T. M., & Fazio, G. 1991, ApJ, 378, 131
Kent, S. M. 1985, ApJS, 59, 115
King, I 1962, AJ, 67, 1303
Kormendy, J. 1977, ApJ, 217, 406
Kormendy, J., Bender, R., Evans, A. S., & Richstone, D. 1998, AJ, 115, 1823
Kormendy, J., & Bruzual A., G. 1978, ApJ, 223, L63
Lauer, T. R., Faber, S. M., Ajhar, E. A., Grillmair, C. J., & Scowen, P. A. 1998, AJ, 116, 2263
Lauer, T. R., et al. 1992, AJ, 104, 552; 1995, AJ, 110, 2622
Michard, R., & Nieto, J.-L. 1991, A&A, 243, L17
Michard, R., & Simien, F. 1988, A&AS, 74, 25
Moles, M., et al., AJ, astro-ph/0504545v1
Naab, T., & Burkert, A. 2001, ApJ, 555, L91
Peng, C. Y. 2002, AJ, 124, 294
Peng, C. Y., Ho, L. C., Impey, C. D., & Rix, H. W., 2002, AJ, 124, 266
Ravindranath, S., Ho, L. C., & Filippenko, A. V. 2002, ApJ, 566, 801
Ravindranath, S., Ho, L. C., Peng, C. Y., Filippenko, A. V., & Sargent, W. L. W. 2001, AJ, 122, 653
Richstone, D., Gebhardt, K., Kormendy, J., Bender, R., Magorrian, J., Sérsic, J. L. 1968, Atlas de Galaxias Australes (Cordoba: Obs. Astron., Univ. Nac. Cordoba)
Shaw, M. A., & Gilmore, G. F. 1989, MNRAS, 237, 903
Simien, F., & Michard, R. 1990, A&A, 227, 11
Tremaine, S., Faber, S., & Lauer, T. 1996, BAAS, 189, 111.02
Tully, R. B. 1988, Nearby Galaxies Catalog (Cambridge: Cambridge Univ.Press)
Tully, R. B., & Fischer, J. R. 1977, A&A, 54, 661
Yee, H. K. C., 1998, AJ, in press, astro-ph/9809347v1